Research Proposal: Rapid Biochemical and Spatial Imaging for Detection and Characterization of Cellular and Sub-Cellular of Bacteria and Spores using Scanning Near-Field Infrared Microscope.

By Omar Trujillo J., PhD and Carl Griffis, PhD
Biological Engineering at the University of Arkansas, Fayetteville, AR

SPECIFIC AIMS

The general objective of this investigation is to build and use a scanning near-field IR microscope (SNFIRM), based on the photo-induced reflectivity principle, to obtain both biochemical and spatial information from cellular and some organelles of bacterial cells *in situ*, and *in vivo.*

Phase I: Build SNFIRM and optimize system's parameters, including resolution, numerical aperture, field of view, image acquisition time, and scanning speed by using created gold patterns on Si substrates.

Phase II: Evaluate operating modes of the SNFIRM by acquiring both point-spectroscopy mode and imaging mode of intact pure culture of *Salmonella typhimurium* cells immobilized in patterned areas on the Si substrate.

Phase III: Evaluate specificity of SNFIRM system by testing multiple bacterial cells, including *Salmonella typhimurium*, three *Staphylococcus strains*, and *Bacillus subtilis* spore. Apply image analysis and statistical methods to differentiate cells by IR spectra and morphology. Sensitivity and identification time will be measured. Add data and Compare with existing FTIR spectra libraries.

BACKGROUND AND SIGNIFICANCE

Background

Analytical methods, such as biochemical imaging, will allow researchers and clinicians to visualize changes in both sample chemistry and morphology *in situ* and *in vivo* under noninvasive conditions. The "fingerprint" spectrum (4-12μm) reflects specific molecular signatures of sample components that are infrared active **(1)**. In particular, bacterial IR spectra contain information of the total composition of the cell (i.e, proteins, polysacharides, nucleic acids, etc), and a combination of spectral windows and mathematical algorithms are used to extract differentiated information **(2)**. Fourier-transform Infrared (FTIR) microscopy and FTIR spectroscopy has been used to detect and characterize bacteria **(2,3)** and spores **(4)**, but these methods have a limited resolution (> 10μm), which prevent them to observe cellular and sub-cellular features commonly observable with visible light microscopes **(5)**. If an object is smaller than one-half the wavelength of the light being used (λ/2), light rays passing by will overlap so much that the object will not be visible. In addition, analysis of biochemical information *in vivo* and in a real-life environment (such as cell organelles, tissues, and fluids) would be very desirable, however both IR

microscopy and FTIR spectroscopy require dehydrated samples. Underwater imaging of thin samples is very difficult to achieve due to the strong water absorption of the IR radiation unless the sample is placed extremely close to the IR source **(6)**. Underwater images of single living cells using a scanning near field infrared microscope (SNIM) with resolutions of $\lambda/4$ have been reported **(6,7)**. *Staphylococcus Aureus* and *Klebsiella pneumoniae* were identified by detecting differences in the "fingerprint" region. However, distance control between the sample and the probe made the system slow (tens of minute per 100x100 image), and complex tip construction and coating was required to avoid degraded resolution. An oscillating tapered tip has been developed to characterize material in the sub-micrometer scale ($\lambda/600$) **(8)**. This approach require dehydrated samples, may suffer from inertial artifacts of the oscillating tip, and like SNIM method, the speed of the system is degraded due to the use of distance control mechanisms. A highly collimated beam of synchrotron radiation could be focused to 3-10μm spots, allowing *in situ* and *in vivo* of bacterial samples **(9,10)**. Synchrotrons produce the full range of electromagnetic spectrum all at once, but they are large and expensive. In the last three years, a new approach is gaining attention: generation of sub-wavelength resolution transient IR probes using photo-induced reflectivity on Si substrates **(11)**. A fast near-field IR microscope providing underwater imaging with 1μm ($\lambda/5$) resolution was reported **(12)**. A further improvement in speed and simplicity was achieved by generating a transient diffractive optical element (Fresnel Lens) in a Si substrate **(13)**. In this investigation, we propose to build and use a scanning near-field IR microscope, based on the photo-induced reflectivity principle, to obtain both biochemical and spatial information from bacterial cells *in situ*, *in vivo*, and using hydrated or dehydrated samples.

Highlights of the system

- *Specificity*: The fingerprint-like pattern obtained from FTIR spectra of bacteria is highly reproducible and specific for different bacteria. Furthermore, distinction between bacterial strains and other strains of the same species will be possible **(2)**. Spectral data libraries such as forensic medicine and pharmaceutical industry will be used to identify unknown samples.
- *Resolution*: $\lambda/5$ .The resolution will be determined by the wavelength of the visible light and its penetration depth into the Si substrate. For example, using blue light and a high numerical aperture (N.A) objective, the spot size can be approximately to 0.4μm in diameter.
- *Multiple bacterial detection:* By immobilizing specific antibodies to a particular bacterial specimen on specific areas of the Si substrate, a computer will differentiate them by IR spectra and location.
- *Viability differentiation:* Different IR spectra will be detected from bacterial cells in their different steps of binary fission. Cell size and morphology will be also detected to complement differentiation.
- *Speed:* A 128x128 image resolution (in pixels) can be acquired in 15 seconds with a 1 KHz repetition laser rate system **(12)**. Further speed is

gained because distance control between sample and probe is not required.

- *Sample preparation*: Intact bacterial cells will be tested. The use of invasive dyes or tags, or extensive sample preparation will not be needed. The sample can be covered by or encased in a transparent liquid or solid **(13)**. To avoid burning the sample, IR pulse energy of several μJ will be produced by either scanning the sample quickly or setting the repetition rate of the IR laser to < 4KHz.

Significance of the Proposed Work

Human Health

The microscope described in this investigation take advantage of two well-known technologies: FTIR spectroscopy and microscopic imaging. The combination of these two methods will provide an useful and affordable tool for clinicians and researchers who will get both biochemical and spatial information of samples *in situ*, *in vivo*, and with the option of having underwater imaging (not possible with existing methods). The use of the system described in this research will facilitate the work biomedical research, such as characterization of biochemical paths and structural changes in cancer and aging. For example, mitochondrion has a size range of 1-5 microns that will fall within the resolution of the SNFIRM. Investigations about mitochondrial pathologies, the role of mitochondria in apoptosis and aging will be benefited because images of mitochondria containing morphological information and localized IR spectra of mitochondira composition will be possible with our system. Mitochondria produce reactive oxygen species (ROS) including superoxide, peroxide, and several nitrogenous species that inhibit or destroy proteins, nucleic acids and lipids **(14)**. Experiments conducted on mutant *Caenorhabditis elegans* worms, showed that *daf-2* longevity gene encoded an insulin receptor-like transmembrane tyrosine kinase, which increased life span from 20 to 55 days (**15**). The stress resistance of these mutant worms was caused by the up-regulation of enzymatic activities that detoxify ROS **(16)**. Understanding in detail the pathways that mediate the benefits of calorie restriction (CR) regimen and that modulate the levels of ROS may lead to novel therapies for a wide range of age related diseases **(14)**.

In general, researchers and clinicians will be able to study of individual human cells, and monitor the stimuli, such as drug uptake, chemicals, or activation or inactivation of processes due to exposure to IR radiation. By studying IR spectra, one can learn how diseases start and spread by understanding the damage and repair mechanisms in living cells.

Justification

The development of rapid methods to recognize and enumerate bacteria is of great value in clinical diagnostics and in the production of foods with the lowest possible numbers of infectious organisms. The potential threat from terrorist groups and the increase in production by food processors has created shipping and storage concerns that require microbiological quality control measures

before they reach consumers. The system described in this research, will be a tool that will contribute to the goal of providing reliable diagnostic analysis of both clinical and food samples performed by private and government agencies. The need for a reliable, sensitive, and rapid method of detection and enumeration of bacteria and spores is evident. In fact, approximately 5 million analytical tests for *Salmonella* are performed in the US per year **(17)**. Furthermore, concerns about the use of bacteria as a weapon, has been reported before the events of September 11 of 2001 **(18).** During Operation Desert Storm, and the recently Operation Enduring Freedom, US troops were exposed to the threat of deadly biowarfare agents such as anthrax, botulinum toxin, and aflatoxin. Recent attacks to civilian populations like those in Florida and the Tokyo subway, also demonstrate the need of a sensitive detection system capable of recognize imperceptible biowarfare agents. For example, *Staphylococcus aureus* Enterotoxin B (SEB) causes nausea, vomiting, and diarrhea when ingested, but causes respiratory distress, irreversible hypotension, shock, and even death if this toxin is acquired in an aerosolized route (**19**). *Yersinia pestis,* the cause of plague and responsible for the deaths of approximately 200 million people throughout history is still active in a number of countries. Economic loses due to food or water contaminated by pathogens such as *Salmonella typhymurium, Eschericia coli, Campylobacter jejuni, Listeria monocytogenes*, among others, have been reported (**20-24**). In fact, one the most dramatic examples are the 1996 incident in which approximately 9000 people fell ill and 313 died as a result of *E. coli O157:H7* contamination and which led to the Hudson ground beef recall in 1997 (**21**). USA zero tolerance standard of less than 1 cell per g sample is pushing food-processing industries to count with rapid, and user-friendly detection and enumeration systems of bacteria. Standard methods for bacteria screening, like plate counting, produces results after 24 h.

RESEARCH DESIGN AND METHODS

Phase I: Building the SNFIRM System

A schematic view of the SNFIRM system is shown in figure 1. Pulsed IR radiation (tunable from 4-10μm) at an energy level of up to 2 μJ will be generated by an optical parametric amplifier (OPA) (Spectra Physics Inc.) and a Ti:Sapphire (Ti:S) laser system. A pump blue (400nm) beam will be generated by the second harmonic of the residual (30%) of the Ti:S laser, and used to produce the photo-induced electron-hole plasma on the 28μ thick Si substrate. A mask with 15 dark and opened zones and projection optics (50X microscope objective) will generate a de-magnified pattern of concentric rings on the lower side of the Si substrate. Shadowed areas will become transparent to IR light-rays while the illuminated ones reflect them. A 600μm size pulsed IR beam will be directed normally to the Si substrate by a small mirror. Under these conditions, the irradiated substrate behaves like a Fresnel lens with its focal point on the upper side of the substrate and with a numerical aperture (N.A.) of about 2.1 **(13)**. An opaque central zone will help to block the zero diffraction order and reduce unwanted background

signals. The sample will be located on the upper side of the Si substrate After transmission through the sample, the IR light will be focused onto a liquid-nitrogen-cooled mercury cadmium telluride detector (KMPV-50, Kolmar Technologies) with a Cassegrainian reflective objective (point-spectroscopy mode) or with a Si/ZnSe lens (Oriel Instruments, inc) system (imaging mode). A high reflactive index Si hemispherical solid immersion lens (h-SIL) is used to maintain $\lambda/5$ resolution and N.A **(25)**. The sample will be located between the Si substrate and the h-SIL. Specific antibodies to the target antigen will be immobilized on patterned areas on the surface of the Si substrate using a thiol-terminal silane and a heterobifunctional crosslinker **(26).** Deep ultraviolet irradiation (DUV) and a photo-mask will be used to alter the size and shape of the capture area so it could be rapidly scanned with the motorized stage (NanoStep17NTS104 with 17MDU002 controller, Melles Griot), of the imaging system.

Optimizing Resolution*:*

In visible light microscopy, the diffraction limitation has been reduced by increasing the refractive index of the media around the sample (i.e., using immersion oil). In the case of IR microscopy, a tiny lens, called solid immersion lens (SIL), is located on top of the sample. Usually Si material is used due to the high index of refraction (n=3.4). We will fabricate h-SIL lenses from single crystal silicon using the techniques described by Fletcher *et. al.* **(25).** A final improved resolution ($>\lambda/5$) will be expected, so that several experiments using different lens diameter will be conducted until an optimum resolution is achieved. As a test sample, 1 μm size polystyrene beads (Polysciences, Inc) will be deposited on a Si substrate, then coated with a thin gold layer. By flushing the beads away, a set of holes will be engraved on the substrate. Next, the edge of one hole will be scanned and the width of the signal transition from 10% to 90% of the amplitude change will determine the final resolution of the system **(12).**

Measuring Field of View (FOV)*:* Once we know the optimum lens diameter, the radius R of the field of view will be calculated:

$$R = \sqrt{\frac{2a\Phi}{n(n-1)\sin^2\theta}}$$

where *a* is the radius of the lens, n is the index of refraction, Φ is the maximum acceptable wave front aberration, and θ is the maximum angle of convergence within the lens **(14).**

Measuring Speed: The stage controller will be setup in such a way that, every step in the X and Y axis will match the size of the Field of view calculated before. Electronic counter connected to a clock circuit will be activated by a trigger signal given by the computer, and deactivated when the final image acquisition has been stored in memory. The speed of the system will be calculated by multiplying the number of pulses counted by the period of the clock circuit.

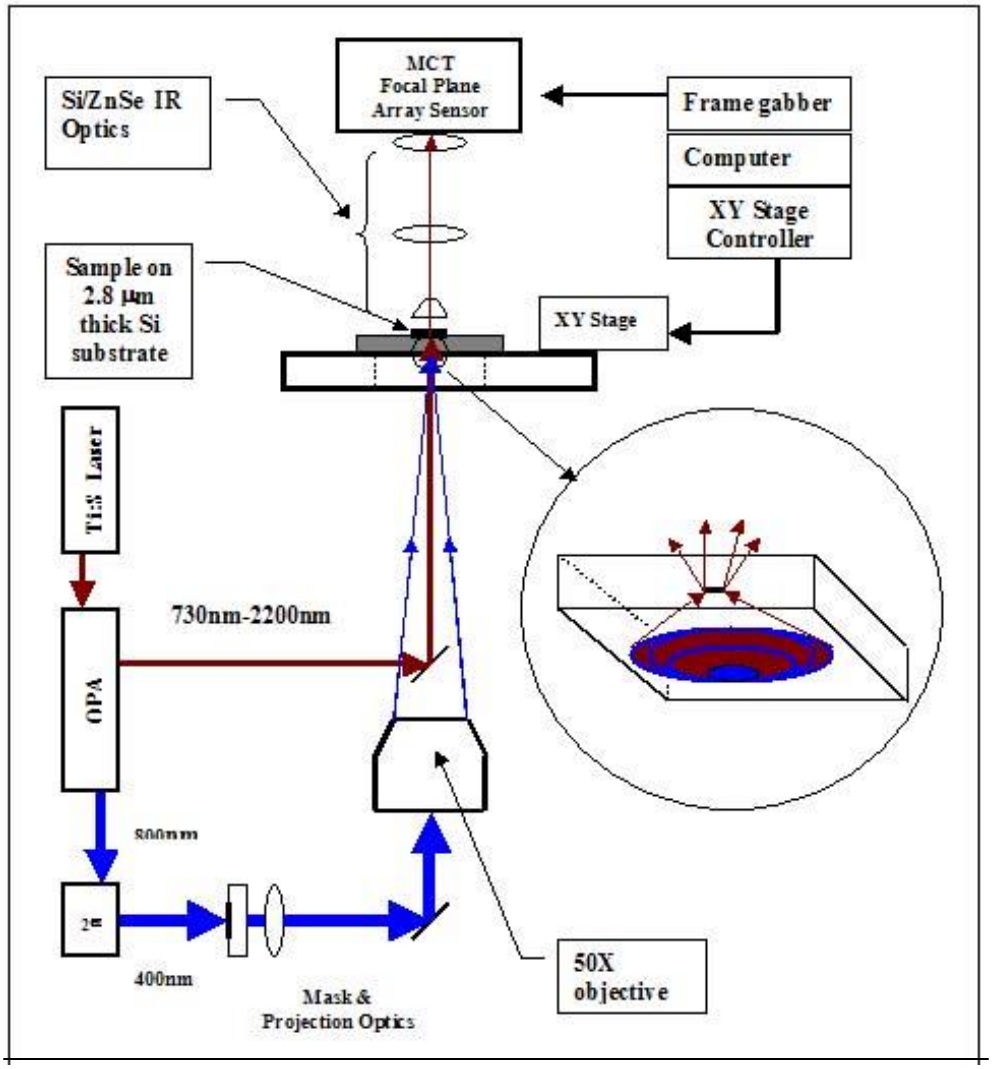

Figure 1. Schematics of the SNFIRM Microscope.

Phase II: System Evaluation.

Preparation of silica substrates

The materials and chemistry for covalent immobilization of antibodies on silica surface, are described in detail by Bathia *et. al*. **(26)**. In summary, the silica surfaces will be cleaned by immersion in a 1:1 mixture of methanol-hydrochloric acid for 30 min followed by several rinses in distilled water and then dried with nitrogen. In a glove bag under an inert atmosphere, the substrates will be treated with a solution of 2% silane (1 ml of 3-mercaptopropyl-triethoxy silane in anhydrous toluene for 12 h). Subsequently, the substrates will be washed three times in toluene, dried on a lint-free cloth, and placed in a clean and dry coplin jar. The size of the capture area will be determined by exposing the silane layer to deep UV light using a $1mm^2$ photo mask. Next, the surfaces will be treated with a heterobifunctional crosslinker (2 mM N-(γ-maleimidobutyryloxy)

succinimide ester in ethanol) for 1 h. Anti-*Salmonella* (75 μl) antibodies will be added then and incubated overnight at 4 °C using a Cone-gene chamber (Electron Microscopy sciences, fort Washington, PA). This procedure will effectively produce a dense layer of capture antibodies on the patterned area (See Figure 2).

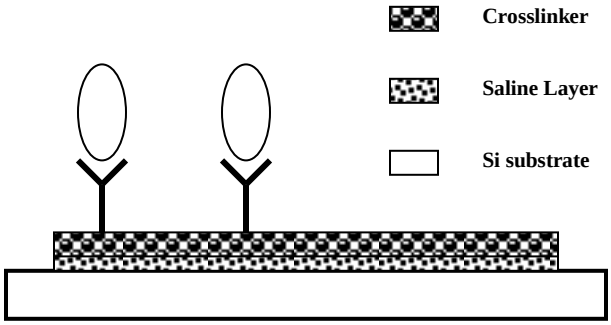

Figure 2. Sample configuration on a Si substrate.

Sample preparation

The slide samples were prepared by a microbiologist in a laboratory located in the Center of Excellence for Poultry Science at the University of Arkansas. Post-chilled whole chicken carcasses were obtained from local processing plants. The carcasses were placed in large bags containing 100 ml of PBS (pH 7.4). The packaged carcasses were shaken and rotated for 1 min on an automatic shaker. The chicken washes were collected and filtered through cheese cloth to remove large chunks of debris. Subsequently, the chicken washes were seeded with *Salmonella typhimurium* and diluted with PBS to a final concentration of $1x10^4$ cfu/ml. A 1-μl sample from dilutions 10^7 to 10^5 will be deposited directly to the capture area on three silica substrates and let the liquid drop dry by placing the substrates in an incubator for 10 min at 37 °C. In theory, 10,000, 1,000, and 100 cells will be present in the substrates respectively, but in the practice, a lower concentration will be expected because not all cells will be captured. A fourth substrate without bacterial cells will be used as a control.

Operation Modes

The SNFIRM will be used in the two operational modes: point-spectroscopy mode and Imaging mode. In the first mode, a Cassegrain reflecting objective (36X , Oriel Instruments) was placed before the IR camera in contrast with the ZnSe lens system used for the second mode. Also, the IR probe will be positioned in one particular point of the sample and the transmission spectrum for that point, will be produced by ramping the laser system over a desired wavelength range. This procedure will be repeated for different points of the sample until the entire sample area is covered. The speed of this mode will be

calculated as described in Phase I, and the time for the formation of 2D image will be expected to be slow.
The imaging mode will produce an image having an area determined by the size of the filed of view at a single wavelength. The stage will be programmed to move in a raster scan mode without overlapping the fields of view until the whole sample area is covered. This procedure will be repeated until a desired wavelength range is scanned. A composite image will be formed by recording in memory all the recorded fields of view and assembling them in the same order as they were acquired. A second composite image will consist of pixels each containing the spectra information of the cellular and organelles of the cells from the first set of composite images. This mode is expected to be faster that the point-spectroscopy mode.

Phase III: Identification of multiple bacterial cells

Preparation of silica substrates
Columns of recognition antibodies on the glass slide will be generated using elastomeric devices and replication molding techniques. Soft elastomeric devices are easy to fabricate, provide good room temperature sealing devices to silica substrates, it has good optical properties, and low material cost **(27).** The elastomeric device will be prepared by casting poly-dimethylsiloxane (PDMS) against a master that has a patterned relief structure in its surface. The master will be fabricated with the help of the High Density Electronic Center at the University of Arkansas by deposition of SIO_2, photoresist, or wax on a silicon wafer after UV exposure through a photomask. A graphical description of multiple bacteria using soft lithography to chemically create recognition antibody patterns and micro-fluidic cambers is shown in Figure 3. A pump will be incorporated to create a rotary flow increase capture performance of the pre-functionalized surface. Following an incubation period of approximately 10 minutes, the elastomeric flow chamber is removed and the slide will be ready for scanning and identification. The computer will operate in imaging mode to discriminate them by IR absorption and column location.

Experimental Design
Two bacterial genera and one spore will be used: *Salmonella typhimurium* (ATCC 14028) and three strains of *Staphylococcus aureus* (ATCC6538), *Staph. epidermis* (DSM20042), and *Staph. hyicus* (DSM20459), and one *Bacillus* spore: *Bacillus subtilis* (ATCC49760). For each of the above, two separate batches will be grown and three spectra will be collected for each batch to yield a total of 30 spectra. In addition, fifteen blind samples will be prepared form various sources including bacteria whose spectra will be in the reference library (see refs **2, 3**), one bacterial cell and spore whose spectra will not be in the library *Listeria monocytogenes* (ATCC BAA-679) and *Bacillus atrophaeus (*ATCC 49337) respectively, and non-bacterial materials whose spectra will not be in the library (i.e., dust, iron oxide, dried grass, and polystyrene). For each blind sample, a single spectrum will be collected as described in Phase II.

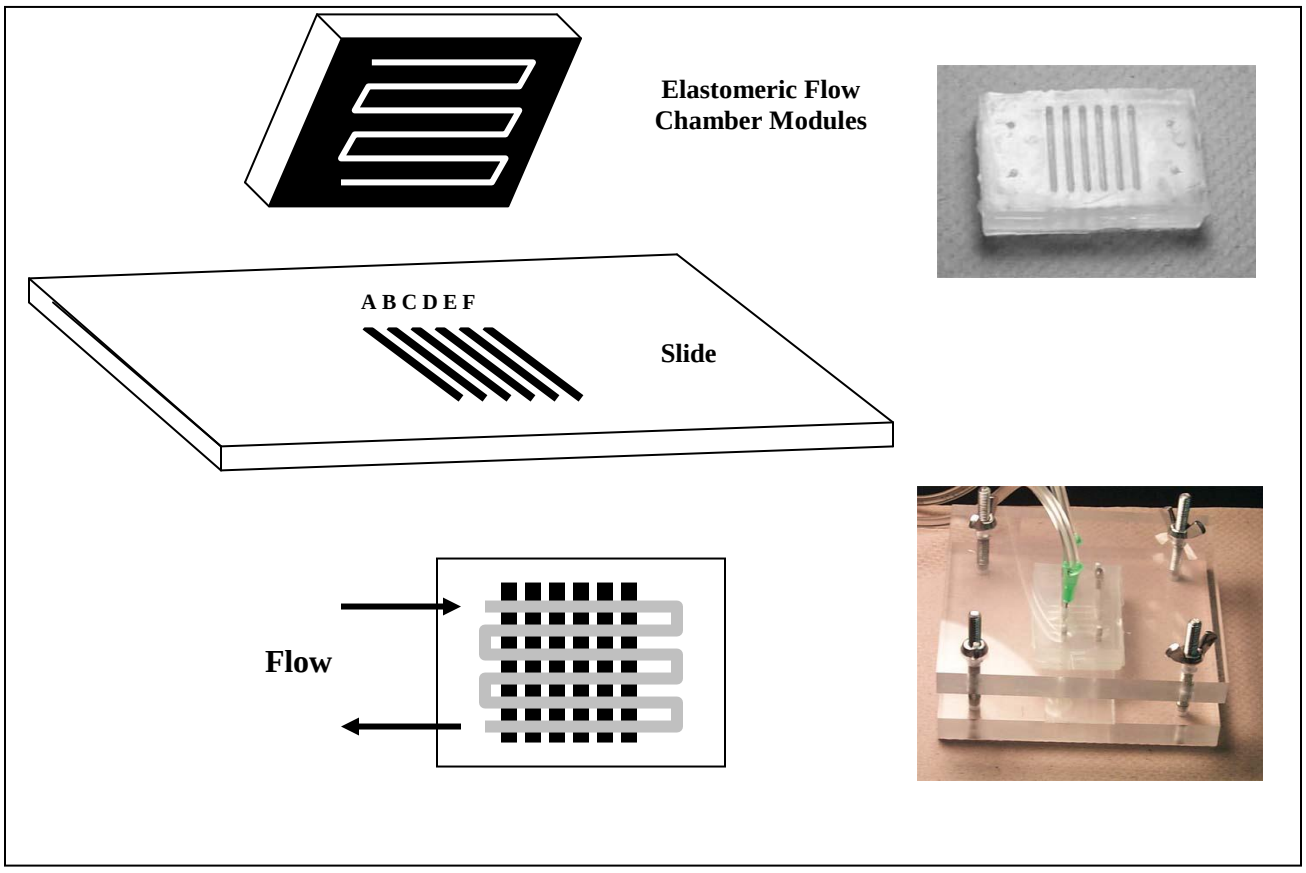

Figure 3. Multiple Identification of Bacterial cells

IR Imaging Processing and Cell Characterization: Statistical Methods

Three techniques will be used to simplify data, compare unknown sample data with reference library, and classify the sample spectra. First Principal component analysis will be used to reduce the dimensionality of the data while retaining the variability in the data. Second, Mahalanobis algorithms willl be used to test similarity of the unknown sample to the training set (library). Finally, Classification and regression trees (CART) will be used to create a decision rule to classify bacterial data. The following flow chart shows the decision approach to identification of bacteria and spores.

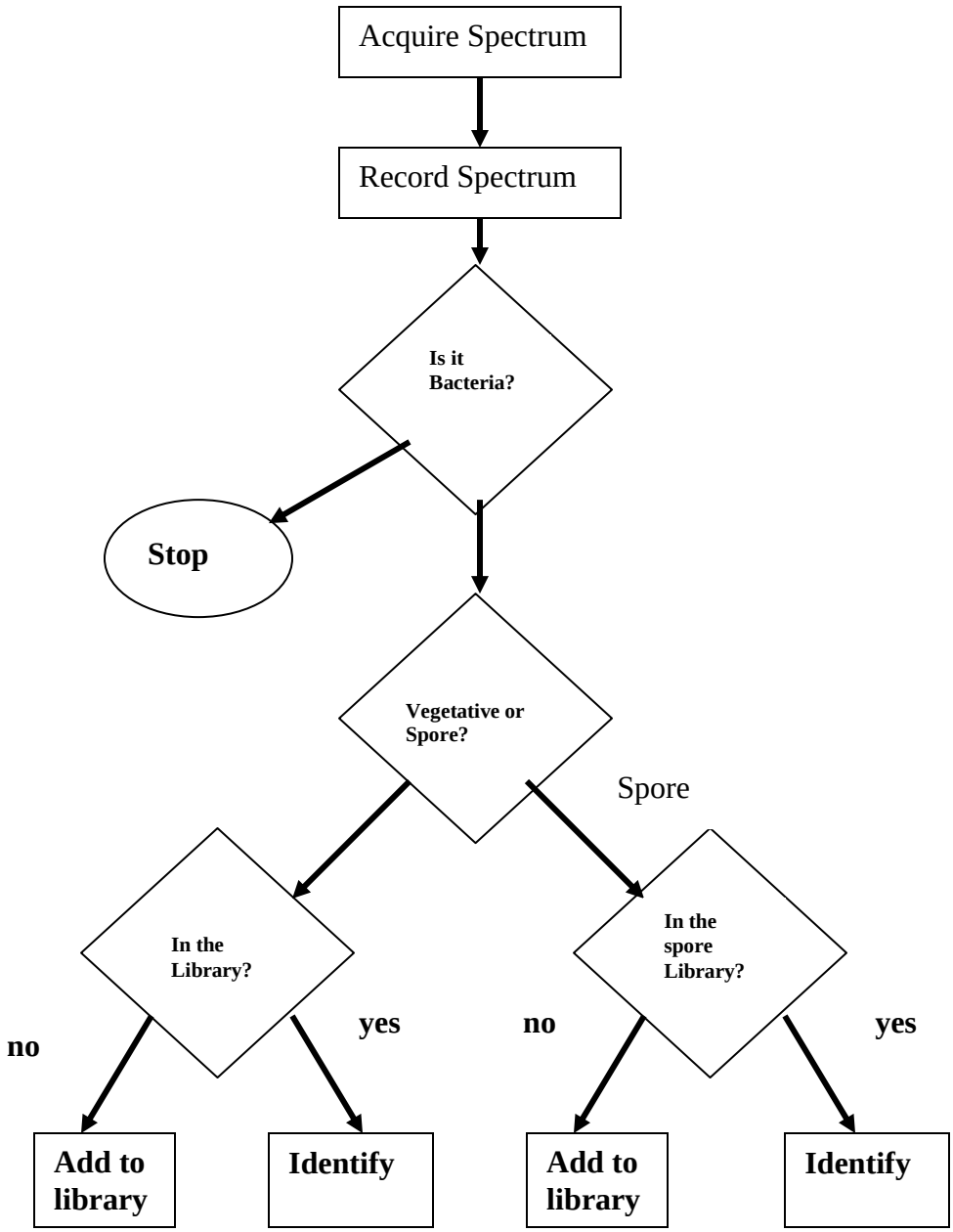

Figure 4. Flow-chart of the decision rules for identification of bacteria.

Image Analysis and Morphology Recognition

A statistical shape recognition algorithm, size, and IR spectra, will be used to train the computer in the recognition of cellular and sub-cellular shapes. Only the sub-cellular structures that fit the resolution of the SNFIRM will be imaged. The purpose of each of the different algorithms described in this section will be the transformation of a video image of a bacterial cell or organelle into a set of shape

descriptors. This transformation requires acquisition of the image, application of image processing techniques such as segmentation, detection of boundary points, centroid calculation, determination of the radius vector, calculation of model parameters, extraction of the feature vector, and pattern recognition.

In this proposal, morphological data from bacterial and spore cells will be generated by the use of circular autoregressive (CAR) model parameters as a representation of the shape of boundaries of digitized images of the cells. The CAR model is used to represent cells's two-dimensional closed contour with a particular form of parametric equation. This approach (Figure 5) will be chosen not only because it is fast, invariant to size and position of the observed object, but also will allow to model convex and concave shapes **(28)**.

A given boundary can be represented by a one-dimensional radii sequence, $\{r(k), 1 \le k \le N\}$, which is composed of the radial distances of N marked-off boundary points from the centroid of the bacteria's shape. In addition, the radius vector lengths will be a function of the angle of projection $\phi = t2\pi / N$, where $t = 1,..., N$. Figure 6 illustrates this boundary representation with mathematical terms.

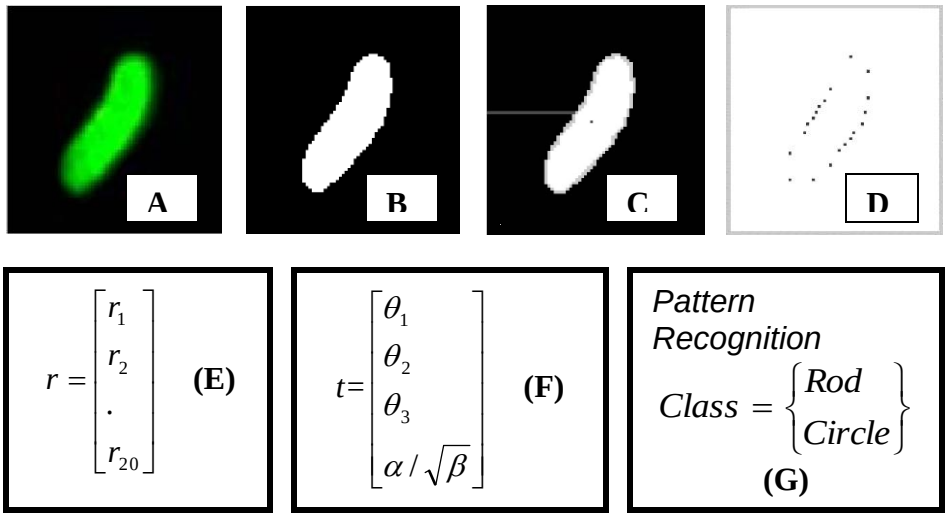

Figure 5. Steps for the recognition of a convex cell shape. (A) Image Acquisition and Flatten Filter. (B) Segmentation. (C) Searching for first boundary pixel, boundary follower, and centroid determination**.** (D) Selection of equally spaced boundary points**.** (E) Create vector with sampled radius distances. (F) Calculation of model parameters and creation of feature vector. (G) Class shape discrimination and decision rule.

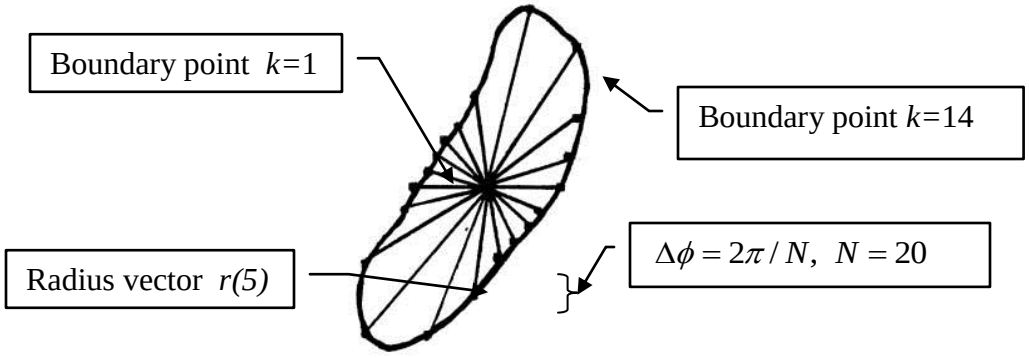

Figure 6. Mathematical boundary representation.

As Figure 7 shows, the ordered set of *k* boundary points will also be expressed as a time series *r(k),* with parameter *k* describing the position of a radius vector in equal angular increments from the starting point. For instance, *r(1)=r(2π/N)* and *r(20)=r(2π).* In order to ensure that the *r(k)* function is single valued, we must ensure that each radius intersects the boundary in only one point. In the case of concave shapes an additional procedure is used **(28).** The optimum N number was determined by performing a one-dimensional FFT on the distances from the centroid to all boundary points. The radius vector number N should be large enough to intersect the boundary at a spatial sampling rate greater than or equal to twice the highest dominant spatial frequency in the boundary spectrum. A routine will be designed to calculate the distance between the centroid and all the boundary points. A boundary radius vector will be created with the radii distances. The coordinates of selected angle values are used to select the corresponding radii from the boundary radius vector. According to Kashyap and Chellappa**.(29),** the $r(k)$ vector can be modeled by a CAR model of the form:

$$r(k) = y(k) + \alpha \ , \qquad y(k) = \sum_{i=1}^{m} \theta_i y(k-i) + \sqrt{\beta w(k)}$$

where: $r(k)$ = current radius vector length

α = the mean value of $r(k)$

$y(k)$ = zero mean sequence

$\theta_i,\ 1 \le i \le m$, = lag coefficients of the zero mean process $y(k)$

$\sqrt{\beta w(k)}$ = e = white noise sequence with variance equal to β

The coefficients $[\theta_{1,\ldots,}\theta_m]$ model the correlated shape variations so that they determine the overall shape of the contour. With the standard least squares method, the parameters of the model can be estimated. The solution for the lag coefficients is obtained by first calculating an estimate of α as the mean value of $r(k)$ and subtracting it from $r(k)$ to obtain the zero mean signal $y(k)$. A

complete description of the calculation of the model parameters is described by Trujillo *et. al.* **(30).**

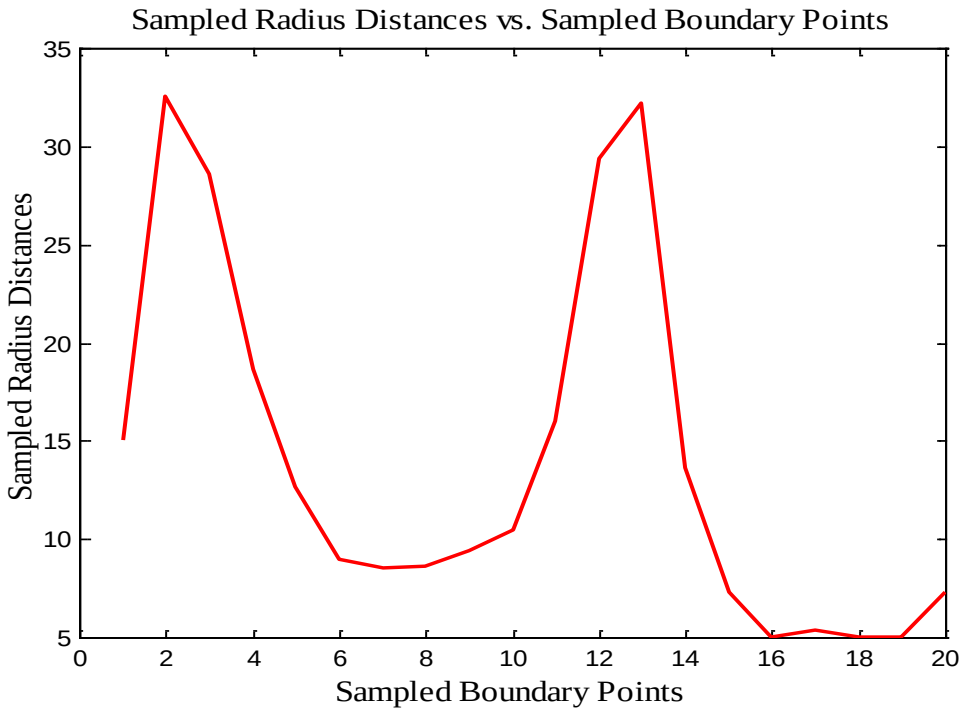

Figure 7. Plot of radii distances vs. sampled boundary points

Feature Vector Determination

The recognition process assigns class membership to an object by comparing its shape descriptors to the shape descriptors of known objects. In this work, two shape classes for cells and spores will be defined: elliptical (rod) shape and circle shapes. The labeled shape descriptors correspond to those calculated by our previous routine, i.e., $[\theta,...,\theta_m, \alpha, \beta]$ and describe representative shapes from different bacteria and spores used as our training set. The training set will consist of ten images of various bacterial cells having the same shape and spores creating a differentiated shape class. Since different bacterial cell will have similar shapes, a further differentiation will be achieved by size and IR spectra. Based upon the methods described by **(28)**, the feature vector, ***t*,** will be chosen to be*:* $t = [\theta_1,...,\theta_m, \alpha/\sqrt{\beta}]$. Since $\sqrt{\beta}$ is related to the noise of the boundary and α is proportional to the shape size, the parameter $\alpha/\sqrt{\beta}$ can be interpreted as a shape signal-to-noise ratio.

Class Shape Discrimination and Decision Rule

A minimum distance classifier called feature weighting (FW), will be used **(31)**. In summary, the FW technique will detect the feature most common to the training set samples and emphasizes that feature in classifying an unlabeled sample. An unlabeled sample will be classified by assigning it to the class whose

cluster of sample points will be closest in the weighted mean square distance sense. The decision rule, which mathematically describes the pattern space partitions, was formed by the classifier training procedure. In this work, a modified version of the FW method, with rotated coordinates (FWR), will be implemented because has better performance. In the FW method, the weights were inversely proportional to the feature standard deviations in the direction of the original coordinate axes. In the FWR method, the class transformations will be expanded to allow a rotation of the coordinate system, as well as scaling of the rotated coordinate system axes. The rotated coordinate system recognition scheme, which forms decision boundaries at the intersection of rotated ellipsoidal contours of constant mean-square distance from the training samples of each class, will place greater emphasis on intra-class similarities than the mean-square intra-class distance in the weighted only pattern space. The feature weights that minimize the intra-class distance in the rotated coordinate method will be:

$$w'_{ii} = \left(\prod_{j=1}^{m+1} \sqrt{\lambda}_j\right)^{1/(m+1)} (1/\sqrt{\lambda}_i), \; i = 1,...,m+1, \quad \text{j=1,…,3}$$

where $\sqrt{\lambda_j} = \sigma_j^{'}$ is the sample standard deviation in the direction of the j[th] sample covariance matrix eigenvector. The covariance matrix will be estimated from the two sample vectors of the class training sets described previously and will have the form:

$$CM = \sum_{i=1}^{m+1} \sum_{k=1}^{m+1} \overline{p_i p_k} - \bar{p}_i \bar{p}_k$$

The eigenvectors ***U*** and eigenvalues λ of the sample covariance matrix will be calculated using the MATLAB (Mathworks, Inc) function [***U***, λ] = ***eig*(CM).** The feature weighting distance equation for the FWR method will be similar to the FW equation but with the difference that, the weights and sample points will be expressed in terms of the rotated coordinate system. The distance, *d(**g**', **C**')*, between an unlabeled vector ***g*** and the cluster of **L** samples of class **C** will be:

$$d(g', C_L') = \sum_{i=1}^{m+1} w'^2_{ii} \left[(g'_{i-} \overline{C}'_i)^2 + \sigma'^2_i\right]$$

where: $\overline{C}'_i$ = is the sample mean vector of the *i[th]* feature expressed in rotated coordinates.

σ'^2_i = is the sample variance in the direction of the j[th] sample covariance matrix eigenvector.

Any vector, for instance the unlabeled vector $g = [g_1 \quad g_2]$ expressed in original coordinates, will be expressed in rotated coordinates by the transformation:

$g' = U^T g = \begin{bmatrix} u_1^T \\ u_2^T \end{bmatrix} g$, where u_1 and u_2 are eigenvectors**.**

Notice that the i^{th} feature weight will be inversely proportional to the standard deviation of the i^{th} training set feature expressed in rotated coordinates. Each eigenvalue, λ_i, will be the variance of the feature points in the direction of the i^{th} eigenvector. An unlabeled sample will be the most heavily set by its similarity to the class mean feature in the direction of the eigenvector with the smallest eigenvalue. The classifier will be trained on each class by calculating the sample covariance matrix and the corresponding eigenvectors and eigenvalues, and calculating the weights and sample mean of each feature of a class training set. For each class, covariance matrices, eigenvectors, eigenvalues, weights, and sample means will be stored in vector form. The sample mean vectors and the unlabeled sample are transformed to the rotated coordinates, and the distance equation is calculated. The decision rule will assign the unlabeled shape to the class corresponding to the smallest distance.

Literature Cited

1. Colthup, N. B., Daly, L.H., and Wiberly, S.E. Introduction to Infrared and Raman Spectroscopy. Academic Press, New York, 1990.
2. Helm, D., Labischinski, H., Schallehn, G., and Naumann, D. Classification and Identification of Bacteria by Fourier-Transform Infrared Spectroscopy. Journal of General Microbiology. 137: 69-79, 1991.
3. Nauman, D., Helm, D., and Labischinski, H. Microbiological Characterizations by FT-IR Spectroscopy, Nature, 351:81-82, 1991.
4. Thompson, S., Foster, N., Johnson, T., Valentine, N., And Amonette, J. Identification of Bacterial Spores Using Statistical Analysis of Fourier Transform Infrared Photoacoustic Specstroscopy Data. Applied Spectroscopy, 57(8):893-899, 2003.
5. Treado, P.J. and Morris, M. D. Infrared and Raman Spectroscopic Imaging, Applied Spectroscopy Reviews, 29(1): 1-38, 1994.
6. Hong, M.K., Jeung, A.G., Dokholyan, N.V., Smith, T.I., and Erramilli, S. Imaging single living cells with scanning near-field infrared microscope based on a free electron laser. Nuclear instruments and Methods in Physics B 144, 246-255, 1998.
7. Erramilli, S., Hong, M.K., and Huie, P., Breaking the Femtogram Barrier Using Scanning Near-field Infrared Microscopy. Proceedings of the SPIE, 3918:197-201, 2000.
8. Lahrech, A., Bachelot, R., Glayzes, P., and Boccara, A.C. Infrared-reflection-mode near-field microscopy using an apertureless probe with a resolution of $\lambda/600$. Optics Letters, 21(17): 1315-1317, 1996.
9. Yee, N., L.G. Benning, M.J. Tobin, and K.O. Konhauser, "Synchrotron Radiation Fourier Transform Infrared Study of Bacteria-water Interactions: Towards a Molecular Understanding of Bacterial Surface Reactivity," in *Proceedings* of Synchrotron Radiation Source User Meeting 2001, September 4-5,2001, Warrington UK.(1.4.3, , ,)
10. Holman, H.N., Martin, M.C., Blakely, E.A., Bjornstat, K., and McKinney, W.R. IR Spectroscopic Characteristics of Cell Cycle Death Probed by

Synchrotron Based Fourier Transform IR Spectroscopy. Biopolymers, 57(6):329-335, 2000.
11. Palanker, D. V., Smith, T. L., and Schwettman, H.A. Fats IR Imaging with Sub-wavelength Resolution Using a Transient Near-Field Probe. SPIE 3605:31-39, 1999.
12. Simanovskii, D., Palanker, K., Cohn, K., and Smith, T. Near-Field infrared microscopy with a transient photo-induced aperture. Applied Physics Letters, 79(8):1214-1216, 2001.
13. Cohn, K., Simanovskii, D., Smith, T., and Palanker, D. Transient photoinduced diffractive solid immersion lens for infrared microscopy. Applied Physics Letters. 81(19): 3678-3680, 2002.
14. Hekimi, S. andGuarente, L. Genetics and Specificity of the Aging Process. Science, 299:1351-1354, 2003.
15. C. elegans daf-2 Sci. Sage KE, GdbGene38; htpp://sageke.sciencemag.org/cgi/genedata/sagekeGdBGene;38.
16. Honda, Y., and Honda, S. FASEB J., 13:1385, 1999.
17. Meng, J. and Doyle, M.P. 1998. Bulletin Institute Pasteur, 96, pp.51.
18. Lee, R., Harbison, R., Hancock, D, Hurt, G., and Draughon, A. August 6, 2000. Bioterrorism and Food Protection. Abstract book:IAFP 87th annual meeting, pp.113.
19. Rowe, C., Scruggs, S., Feldstein, M., Golden, J., and Ligler, F. 1999. An Array Immunosensor for Simultaneous Detection of Clinical Analytes. Analytical Chemistry, Vol. 71, No.2, 433-439.
20. Tanaka, Y., N.Yamaguchi, and M. Nasu. 2000. Viability of *Escherichia coli* O157:H7 in natural river water determined by the use of flow cytometry. J Appl Microbiol. 88(2):228-36.
21. USDA, August 12, 1997. Hudson Foods recalls beef burgers nationwide for *E. coli O157:H7*, News Release No. 0272.97, Washington, DC.
22. USDA-FSIS. Jan. 22, 1999. Thorn Apple Valley Frankfurters and lunch combination products recalled for potential *Listeria* contamination. http://www.fsis.usda.gov/OA/recalls/prelease/pr005-99.htm
23. USDA-FSIS. Jan. 22, 1999. BIL MAR Listeria recall—Additional brands sold at retail. http://www.fsis.usda.gov/OA/recalls/prelease/pr044-98a.htm
24. USDA-FSIS. Oct. 30, 1998. Florida firm expands recall of franks for *Listeria*. http://www.fsis.usda.gov/OA/recalls/prelease/pr035-98b.htm
25. Flecher, D.A., Crozier, K.B., Quate, C.F., Kino, G.S., and Goodson, K.E. Refraction Contrast Imaging with a Scanning Microlens. Applied Physics Letters, 78(23):3589-3591, 2001.
26. Bhatia, S. K., Shriver, L. C., Prior, K. J., Georger, J. H., Calvert, J.M., Bredehorst, R., and Ligler, F.S. Use of Thiol-Terminal Silanes and Heterobifunctional Crosslinkers for Immobilization of Antibodies on Silica Surfaces. Analytical Biochemistry, 178:408-413, 1989.
27. Xia, Y. and Whitesides, G.M., Soft Lithography. Angewandte Chemie Int. Ed., 37:550-575, 1998.

28. Dubois, S. R. and Glanz, F. H., An Autoregressive Model Approach to Two-Dimensional Shape Classification. *IEEE Transactions On Pattern Analysis And Machine Intelligence*, 8(1):55-65, 1986.
29. Kashyap, R.L. and Chellappa, R. Stochastic Models for Closed Boundary Analysis:Representation and Reconstruction. *IEEE Transaction on Info Theory*, 27(5):627-637, 1981
30. Trujillo, O Bioimaging Analysis for rapid Recognition of Pathogens on Poultry Materials. MS Thesis: University of Arkansas, Fayetteville,2000.
31. Trujillo, O., Griffis, C., Li, Y., and Slavik, M. 2001. A Machine Vision System Using Immuno-Fluorescence Microscopy For Rapid Recognition of *Salmonella typhimurium*. *Journal of Rapid Methods and Automation in Microscopy*. 9:115 -134, 2001.